Multiband superconductivity in $LaFeAsO_{0.9}F_{0.1}$ single crystals probed by high-field vortex torque magnetometry

G. Li,[1] G. Grissonnanche,[1] A. Gurevich,[1,*] N. D. Zhigadlo,[2] S. Katrych,[2] Z. Bukowski,[2] J. Karpinski,[2] and L. Balicas[1,†]

[1]*National High Magnetic Field Laboratory, Florida State University, Tallahassee, Florida 32310, USA*

[2]*Laboratory for Solid State Physics, ETH Zürich, CH-8093 Zürich, Switzerland*

(Received 18 January 2011; revised manuscript received 30 March 2011; published 3 June 2011)

To probe manifestations of multiband superconductivity in oxypnictides, we measured the angular dependence of the magnetic torque $\tau(\theta)$ in the mixed state of $LaO_{0.9}F_{0.1}FeAs$ single crystals as a function of temperature T and magnetic fields H up to 18 T. The paramagnetic contribution of the Fe ions is properly treated in order to extract the effective mass anisotropy parameter $\gamma = (m_c/m_{ab})^{1/2}$ from $\tau(\theta)$. We show that γ depends strongly on both T and H, reaching a maximum value of $\sim$10 followed by a decrease toward values close to 1 as T is lowered. The observed field dependencies of the London penetration depth λ_{ab} and γ suggest the onset of suppression of a superconducing gap at $H \approx H_{c2}/3$.

DOI: 10.1103/PhysRevB.83.214505 PACS number(s): 74.25.Ha, 74.25.Op, 74.70.Xa

I. INTRODUCTION

The recently discovered superconducting oxypnictides[1,2] have similarities with the high-T_c cuprates, such as the emergence of superconductivity upon doping a parent antiferromagnetic compound.[2–4] Theoretical models[5] suggest unconventional $s^{\pm}$ pairing, consistent with Andreev spectroscopy,[6] penetration depth,[7] and photoemission measurements[8] which indicate nodeless s-wave pairing symmetry. Experiments at high magnetic fields,[8–10] penetration depth,[7,11,13] and heat capacity measurements[12] are consistent with the multiband $s^{\pm}$ scenario.[5] Other models suggest an important role for electronic correlations,[14] and even a possibility of unconventional pairing mechanisms.[15]

The comparatively high critical temperatures T_c and extremely high upper critical fields H_{c2} of the oxypnictides[9,16] indicate their promising prospects for applications if, unlike the layered cuprates, a sizable vortex liquid region does not dominate their temperature–magnetic field (T-H) phase diagram. It is therefore important to reveal the true behavior of the anisotropic magnetization in the vortex state of the oxypnictides, particularly the extent to which vortex properties are affected by strong magnetic correlations and multiband effects. For instance, multiband effects in MgB_2 can manifest themselves in strong temperature and field dependencies for the mass anisotropy parameter $\gamma(T,H) = (m_c/m_{ab})^{1/2}$ and the London penetration depth $\lambda(T,H)$ even at $H \ll H_{c2}$.[17,18] Similar effects in pnictides would be consistent with the multiband pairing scenarios.[5] Yet, there are significant differences between two-band superconductivity in MgB_2 and in oxypnictides: In MgB_2 the interband coupling is weak, while in the oxypnictides it is the strong interband coupling which is expected to result in the high T_c.[5] Thus, probing multiband superconductivity in oxypnictides by magnetization measurements requires high magnetic fields, which can suppress the superfluid densities in both bands by circulating vortex currents. In this work we address these issues, presenting high-field torque measurements of the anisotropic reversible magnetization in $LaFeAsO_{0.9}F_{0.1}$ single crystals. Our measurements of $\gamma(T,H)$ up to 18 T and extended temperature range, $4 < T < 15$ K, reveals a different behavior in $\gamma(T,H)$ as compared to recent low-field torque measurements.[10] Reference 10 shows a γ that increases continuously as T is lowered reaching a maximum value of $\sim$20 for both $NdFeAsO_{0.8}F_{0.2}$ and $SmFeAsO_{0.8}F_{0.2}$ single crystals. In contrast, our results indicate that γ in $LaFeAsO_{0.9}F_{0.1}$ reaches a maximum of $\sim$10 decreasing asymptotically toward 1 as T is lowered.

Measurements of the equilibrium magnetization $m(T,H)$ of the vortex lattice in $LaO_{0.9}F_{0.1}FeAs$ are complicated by the smallness of $m(T,H)$ caused by the large Ginzburg-Landau parameter, $\kappa = \lambda/\xi > 100$, and by the background paramagnetism of the normal state,[19] which can mask the true behavior of $m(T,H)$. In this case torque magnetometry is the most sensitive technique to measure the fundamental anisotropy of the parameters of $\vec{m}(T,\vec{H})$ in small single crystals. The torque $\vec{\tau} = \mu_0 \vec{m} \times \vec{H}$ acting upon a uniaxial superconductor is given by

$$\tau(\theta) = \frac{HV\phi_0(\gamma^2-1)\sin 2\theta}{16\pi\mu_0\lambda_{ab}^2\gamma^{1/3}\varepsilon(\theta)} \ln\left[\frac{\eta H_{c2}^{ab}}{\varepsilon(\theta)H}\right] + \tau_m \sin 2\theta, \quad (1)$$

where V is the sample volume, ϕ_0 is the flux quantum, H_{c2}^{ab} is the upper critical field along the ab planes, $\eta \sim 1$ accounts for the structure of the vortex core, θ is the angle between $\vec{H}$ and the c axis, $\varepsilon(\theta) = (\sin^2\theta + \gamma^2\cos^2\theta)^{1/2}$, and $\gamma = \lambda_c/\lambda_{ab}$ is the ratio of the London penetration depths along the c axis and the ab plane. The first term in Eq. (1) was derived by Kogan in the London approximation valid at $H_{c1} \ll H \ll H_{c2}$,[20] while the last term describes the torque due to the background paramagnetism, for which $\tau_m = \mu_0(\chi_c - \chi_a)VH^2/2$ and χ_c and χ_a are the normal-state magnetic susceptibilities along the c axis and ab plane, respectively. In general, $\gamma = (m_c/m_{ab})^{1/2} \neq \lambda_c/\lambda_{ab}$, (where m_c and m_{ab} are the Ginzburg-Landau superconducting effective masses) but both ratios are assumed to be equal in the model leading to Eq. (1). As will be shown below, the paramagnetic term in Eq. (2) in $LaO_{0.9}F_{0.1}FeAs$ can be larger than the superconducting torque, which makes extraction of the equilibrium vortex magnetization nontrivial. In this work we propose a method which enables us to resolve this problem and measure the true angular dependence of the superconducting torque as a function of both $\vec{H}$ and T, probing the concomitant behavior

of $\gamma(T,H)$ and $\lambda_{ab}(T,H)$ and manifestations of multiband effects.

II. EXPERIMENTAL

Underdoped single crystals of $LaO_{1-x}F_xFeAs$ with typical sizes of $80 \times 60 \times 5$ μm^3 were grown by the flux method described in Ref. 21. The samples had a critical temperature $T_c \simeq 15$ K as determined by the SQUID magnetometry, and as shown in Fig. 1. The width of superconducting transition, measured by a commercial SQUID magnetometer under a field $H = 10$ Oe after cooling the crystal under zero field, is $\Delta T_c \sim 3.5$ K. This relatively broad transition may not reflect the sample quality but mostly results from the penetration of vortices in a platelike crystal which has a large demagnetization factor and thus reduced lower critical field, although in some crystals from the same batch the width of the resistive transition, from the very onset of the resistive transition to the zero resistance state, is observed to be as large as $\Delta T \simeq 3$ to 4 K, consistent with the values reported in the literature for crystals with similar composition.[22] The fraction of F quoted here corresponds to a nominal value since its precise content is very difficult to determine in such small single crystals. However, a superconducting transition temperature $T_c \simeq 15$ K, see Fig. 1, firmly places these crystals within the underdoped state, following the overall phase diagram displaying $T_c(x)$ as a function of the F content x.[24] As argued in Ref. 23, F is expected to be inhomogeneously distributed throughout the samples.

Samples were attached to the tip of a piezo-resistive micro-cantilever placed in a rotator inserted into a ^{3}He cryostat. The ensemble was placed into a 18 T superconducting solenoid. Changes in the resistance of the micro-cantilever associated with its deflection and thus a finite magnetic torque τ was measured via a Wheatstone resistance bridge.

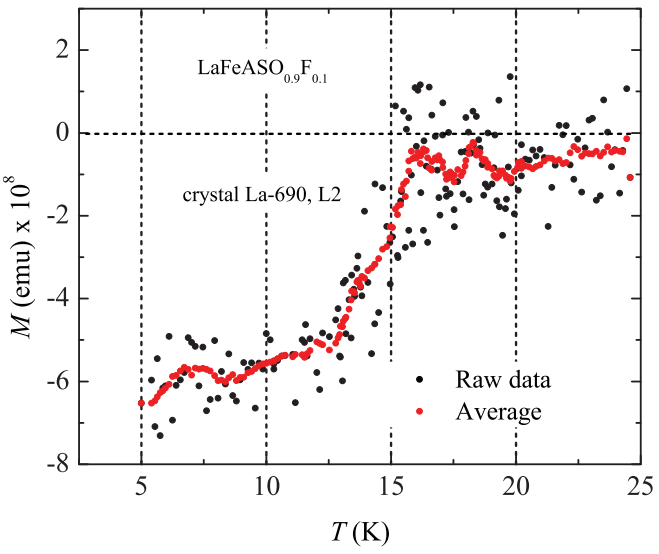

FIG. 1. (Color online) (a) Magnetization M as a function of temperature for a typical $LaO_{0.9}F_{0.1}FeAs$ single crystal measured under an external field of 10 Oe. The small mass of the single crystal, of just a few micrograms, leads to the observed large scattering in the data points. Red markers correspond to $M(T)$ averaged over 20 raw data points.

III. RESULTS AND DISCUSSION

Figure 2(a) shows the angular dependence of the torque $\tau(\theta)$ at $T = 8$ K and under $H = 5$ T for a $LaFeAsO_{0.9}F_{0.1}$ single crystal. Hysteresis, resulting from the irreversible magnetization due to vortex pinning, is observed between increasing and decreasing angular sweeps. The black line depicts the average value of both traces, $\tau_{rev}(\theta) = [\tau(\theta)_{up} + \tau(\theta)_{down}]/2$, defined as an equilibrium magnetization, where θ_{up} and θ_{down} indicate either increasing or decreasing angle sweeps, respectively. This reversible torque contains both superconducting and paramagnetic contributions. Given that vortex pinning and concomitant hysteresis are bound to disturb the equilibrium magnetization, we have checked that our definition of $\tau_{rev(\theta)}$. leads to reproducible traces, by remeasuring $\tau(\theta)$ for both θ_{up} and θ_{down} within two distinct angular ranges, as shown in Figs. 2(b) and 2(c). The respective $\tau_{rev}(\theta)$ traces, i.e., blue and magenta traces, are plotted in Fig. 2(d) together with the original $\tau_{rev}(\theta)$ from Fig. 2(a). As seen, all traces overlap almost perfectly. Both sharp spikes seen at either side of $\theta = 90^\circ$ are likely due to pinning effects.

Figure 3(a) shows the angular dependence of the torque $\tau(\theta)$ at $T = 10$ K and $H = 5$ T for a *second* $LaFeAsO_{0.9}F_{0.1}$ single crystal. In this crystal and at this temperature one does not observe any structure that might be attributable to pinning and which would compromise a fit attempt of the resulting $\tau_{rev}(\theta)$ (brown line) to either Eq. (1) or Eq. (2). As shown in Fig. 3(b), the paramagnetic term $\tau_m \sin 2\theta$ increases rapidly as the field increases, preventing a direct fit of $\tau_{rev}(\theta)$ to Eq. (1) since $\tau_m \sin 2\theta$ interferes with the $\sin 2\theta$ harmonics of the first term. Yet the superconducting parameters $\gamma(T,H)$ and $\lambda(T,H)$ can be unambiguously extracted from the data adding a 90° translation of $\tau_{rev}(\theta)$ to itself, i.e., $\tau_{rev}(\theta) + \tau_{rev}(\theta + 90^\circ)$, where the paramagnetic term in $\tau(\theta)$ cancels out:

$$\tau_+ = \tau(\theta) + \tau(\theta + 90^\circ) = \frac{V\phi_0(\gamma^2 - 1)H \sin 2\theta}{16\pi\mu_0\lambda_{ab}^2\gamma^{1/3}} \times \left[\frac{1}{\varepsilon(\theta)} \ln\left(\frac{\eta H_{c2}^{ab}}{\varepsilon(\theta)H}\right) - \frac{1}{\varepsilon^\star(\theta)} \ln\left(\frac{\eta H_{c2}^{ab}}{\varepsilon^\star(\theta)H}\right)\right], \quad (2)$$

where $\varepsilon^\star(\theta) = (\cos^2\theta + \gamma^2 \sin^2\theta)^{1/2}$. This procedure is illustrated in Fig. 3(c), which shows $\tau_+(\theta)$ as a function of θ for all curves in Fig. 3(b). Notice that the amplitude of $\tau_+(\theta)$ is considerably smaller than that of $\tau_{rev}(\theta)$.

Since $\tau_+(\theta)$ in Eq. (2) depends on three fit parameters, γ, λ, and ηH_{c2}, different sets of parameters may give equally good descriptions of the experimental data. One can circumvent this difficulty by extracting ηH_{c2} from the amplitude of $\tau_+(\theta)/H$ plotted as a function of $\ln(1/H)$ for several values of θ, as shown in Fig. 4(a). If at a given temperature, these measurements are performed up to high enough fields, the extrapolation of $\tau_+(\theta)/H$ to zero evaluates the value $H_\star$ at which $\eta H_{c2}^{ab}/\varepsilon(\theta)H_\star = 1$. From the two extrapolated values of $H_\star$ for $\theta_1 = 110^\circ$ and $\theta_2 = 120^\circ$, we exclude γ and obtain $(\eta H_{c2})^2 = H_\star^2(\theta_1)H_\star^2(\theta_2)\sin(\theta_2 - \theta_1)\sin(\theta_2 + \theta_1)/[H_\star^2(\theta_1)\cos^2\theta_1 - H_\star^2(\theta_2)\cos^2\theta_1]$, which yields $\eta H_{c2}^{ab} \simeq 27$ T for $T = 10$ K. This simple method provides a

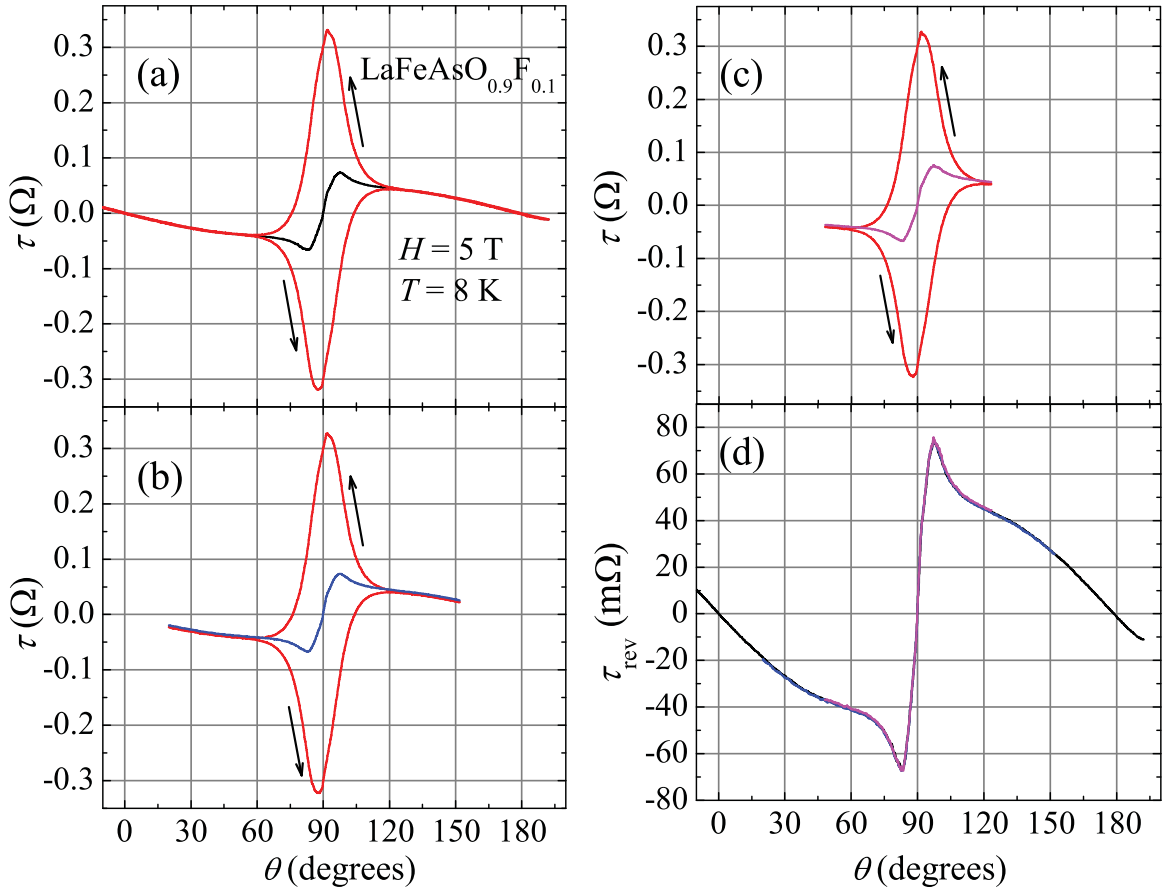

FIG. 2. (Color online) (a) Magnetic torque τ for a $LaO_{0.9}F_{0.1}FeAs$ single crystal for increasing and decreasing angle (θ) sweeps (red lines), at $H = 5$ T and $T = 8$ K. Arrows indicate either increasing (θ_{up}) or decreasing (θ_{down}) angles. Black line is the reversible torque component or $\tau_{rev}(\theta)$ defined here as the average between both traces. (b) Same as in (a) but in a smaller angular range. (c) Same as in (a) and in (b) but in an even shorter angular range. (d) The resulting $\tau_{rev}(\theta)$ from (a), (b), and (c).

thermodynamic estimate for H_{c2}^{ab} without the need of extremely high magnetic fields, $H \simeq H_{c2}(\theta)$. Furthermore, with $\eta H_{c2}^{ab} \simeq 27$ T we obtain excellent and stable two-parameter fits of $\tau_+(\theta)$ to Eq. (2) for virtually all field values, as shown in Fig. 4(b). Here the parameters γ and λ no longer interfere in the fit as λ affects only the magnitude but not the shape of $\tau_+(\theta)$. We confirmed that the extracted parameters lead to a small difference in the logarithmic terms of Eq. (2) at $H = H_\star$.

Using the method outlined above, we extracted the field and the temperature dependencies of $\gamma(T,H)$, $\lambda_{ab}(T,H)$. An example is given by the orange line in Fig. 5(a) for $H = 6$ T and $T = 10$ K. Having fixed γ, λ, and ηH_{c2}^{ab} we can now fit the original $\tau_{rev}(\theta)$ to Eq. (1) (red line), leaving the amplitude of the paramagnetic component τ_m as the only adjustable parameter (magenta line). Figure 5(b) depicts the resulting amplitudes for both τ_m and the superconducting contribution $\tau_K \propto H/\lambda_{ab}^2$ in Eq. (1) as a function of field for $T = 10$ K. The amplitude of τ_K follows the expected linear in field dependence up to $H = 8$ T, from which point it starts to decline continuously. On the other hand, τ_m follows the expected H^2 dependence characteristic of the torque of an anisotropic paramagnetic background. To our knowledge, this is the first magnetometry method which allows an independent extraction of the parameters of a magnetic superconductor.

The curves $\tau(\theta)$ measured for $T > 4$ K indicate that $\eta H_{c2}^{ab}(T)$ is described by $\eta H_{c2}^{ab}(T) = \eta H_{c2}^{ab}(0)[1-(T/T_c)^2]$. As seen in Fig. 5, the irreversible component in $\tau(\theta)$ grows quickly as the temperature is lowered. At $T = 4$ K despite the observed large irreversibility, the resulting reversible component in $\tau(\theta)$ is still nearly perfectly described by Eq. (1), see Fig. 6(a). However, as the temperature is lowered to $T = 1.5$ K additional structures emerge in $\tau(\theta)$ for θ close to 90°, see Fig. 6(b). We ascribe these features to the intrinsic pinning of vortices by the planar structure of the material, which prevents a reliable extraction of the reversible component in $\tau(\theta)$ below $T \sim 4$ K. A detailed analysis and discussion will be provided elsewhere.[25]

Figure 7(a) shows the resulting temperature dependence of the total superfluid density $n_s \propto \lambda_{ab}^{-2}$ measured under a field $H = 5$ T. A field of 5 T is high enough to suppress the irreversible component in the torque as compared to the reversible one, and to neglect demagnetization factors and geometrical barriers for the penetration of magnetic flux through the sample. Our torque magnetometer was not calibrated, so we could only measure the temperature dependency of $\lambda_{ab}(T)$ but not the absolute values of λ_{ab} or n_s. Despite the unavailability of points at the lowest T's, the temperature dependence of $n_s(T)$ exhibits a positive curvature as seen in penetration depth

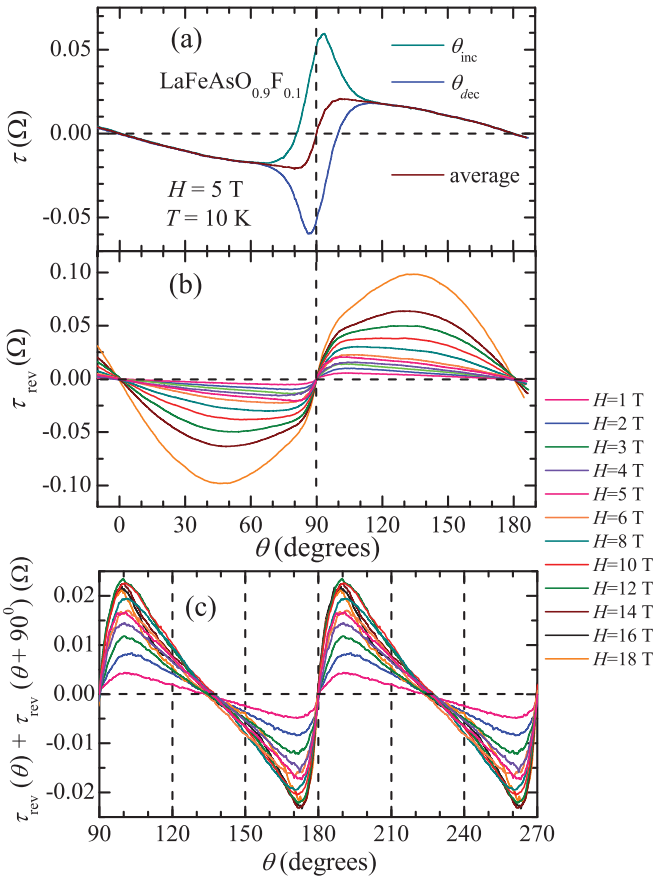

FIG. 3. (Color online) (a) Magnetic torque τ for a $LaO_{0.9}F_{0.1}FeAs$ single crystal for increasing (clear blue line) and decreasing (blue line) angle (θ) sweeps, at $H = 3$ T and $T = 27$ K. (b) $\tau_{rev}(\theta)$ for several field values at $T = 10$ K. (c) The symmetrized component $\tau_{rev}(\theta) + \tau_{rev}(\theta + 90^\circ)$ of the torque due solely to the reversible vortex magnetization.

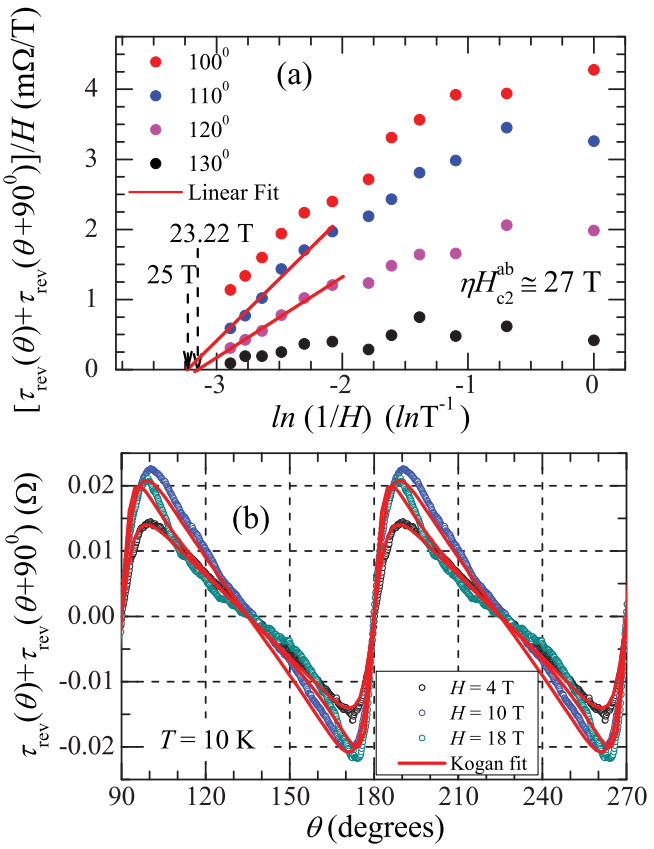

FIG. 4. (Color online) (a) The amplitude of $[\tau_{rev}(\theta) + \tau_{rev}(\theta + 90^\circ)]/H$ as a function of $\ln(H^{-1})$ for several angles, taken from the data in Fig. 3(c). Red lines are linear extrapolations of $[\tau_{rev}(\theta) + \tau_{rev}(\theta + 90^\circ)]/H \to 0$ for $\theta = 110^\circ$ and 120°, which yields $\eta H_{c2}^{ab} \simeq 27$ T for $LaFeAsO_{0.9}F_{0.1}$ at $T = 10$ K. (b) With the value $\eta H_{c2}^{ab} \simeq 27$ we obtain excellent fits of $\tau_{rev}(\theta) + \tau_{rev}(\theta + 90^\circ)$ to Eq. (2) for all field values.

measurements in the compounds $RFeAsO_{0.9}F_{0.1}$ (R=La, Nd, with T_c's of 14 and 45 K, respectively).[26] But it contrasts with penetration depth results for $PrFeAsO_{1-y}$ ($T_c \simeq 35$ K)[27] and for $SmFeAsO_{0.8}F_{0.2}$ ($T_c \simeq 44$) K,[7] which finds evidence for a superconducting state characterized by more than one (non-nodal) gap. In Ref. 26 such an upward curvature was explained in terms of the $s^{\pm}$ scenario, with the superconducting gap ratio $\Delta_1/\Delta_2 \simeq 1/3$. As follows from Fig. 7(b), the associated $\lambda_{ab}(T)$ in our limited temperature range follows a T^2 dependence at low and intermediate temperatures, in contrast to the linear dependence expected for a nodal gap as observed in LaFePO,[28] or the nearly exponential behavior expected for a clean s-wave superconductor, as reported for $SmFeAsO_{0.8}F_{0.2}$[7] and $PrFeAsO_{1-y}$.[27] One important debate concerning the Fe arsenides is precisely the origin of these differences, since a common pairing mechanism[5,14] has been proposed for all compounds based on the presumed similarity of their electronic structure. At the same time, it was recently argued that the extended s-wave scenario can lead to either nodeless or nodal gaps, depending on the interplay between intraband and interband interactions.[29] Penetration depth measurements over an extended region in reduced temperatures (T/T_c) also revealed a T^2 dependence for λ_{ab} in $RFeAsO_{0.9}F_{0.1}$ (R = La, Nd)[26] as well as in $Ba_{1-x}K_xFe_2As_2$.[13] This power-law temperature dependence was deemed to be consistent with the $s\pm$ multigap scenario, if either strong interband impurity scattering[30] or pair-breaking effects[31] are important. Our observation of a $n_s \propto T^2$ is limited by the restricted temperature range imposed by the pinning effects at lower T's, yet we believe that it is important to expose the agreement for the anomalous temperature dependence of the penetration depth between magnetic torque and surface impedance measurements in the case of $LaFeAsO_{0.9}F_{0.1}$. Given the width of the superconducting transition ≃3–4 K, it is possible that local variations of T_c due to an inhomogeneous distribution of F could affect the dependence of n_s on T at higher temperatures. In addition, given that our measurements of $n_s(T)$ were performed under a field of 5 T, we cannot completely rule out that the temperature dependence of $H_{c2}(T)$ might influence the power-law dependence for $n_s(T)$ reported here, particularly at higher temperatures.

Figure 7(b) also displays the temperature dependence of the mass anisotropy parameter γ, which starts at $\gamma \simeq 7$ for $T \leqslant T_c$, increases toward a maximum of ∼10 at $T \simeq 0.75\ T_c$, and then decreases to ≈1 as T is lowered (as happens in

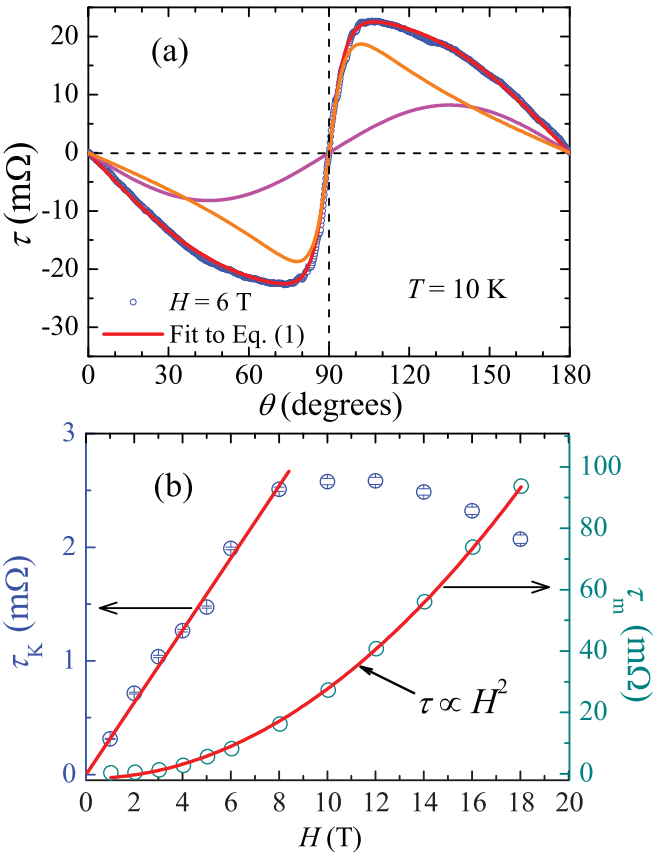

FIG. 5. (Color online) (a) Reversible torque $\tau_{rev}(\theta)$ for a $LaFeAsO_{0.9}F_{0.1}$ single crystal (blue markers) at $H = 6$ T and $T = 10$ K. Orange line shows the reversible vortex torque τ_K and the magenta line shows the paramagnetic torque extracted from the data shown in Fig. 3 using the deconvolution procedure described in the text. Red line shows the sum of τ_K with the paramagnetic term. (b) The amplitude of τ_K normalized by $(\gamma^2 - 1)/\gamma^{1/3}$ (blue markers) and that of the paramagnetic term (clear blue markers) as functions of H. At lower fields, $\tau_K(H,\theta)$ increases linearly with H, while the paramagnetic term exhibits a H^2 dependence.

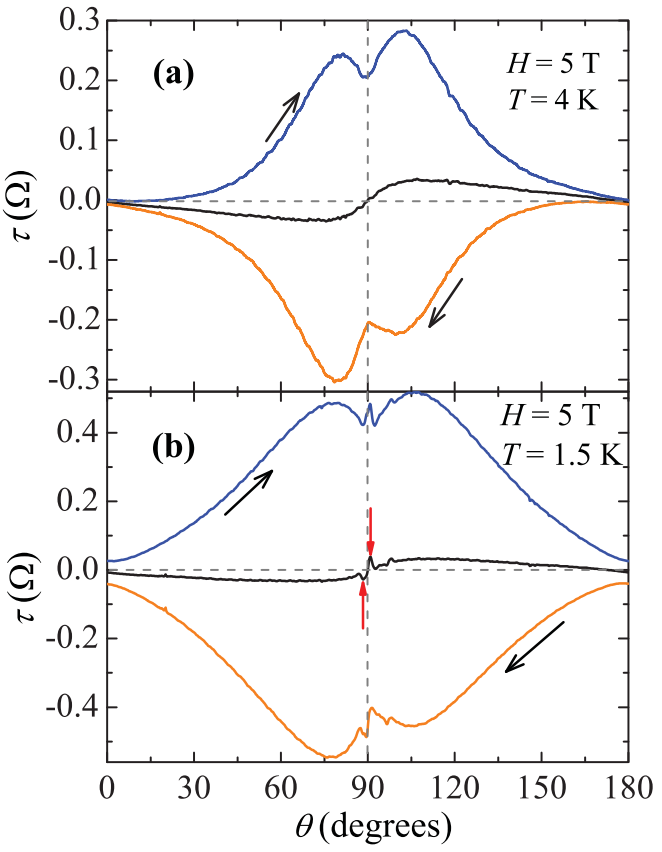

FIG. 6. (Color online) (a) τ as a function of the angle θ and respectively for increasing (blue line) and decreasing (orange line) angle scans at $T = 4$ K and under a field $H = 5$ T. Black line corresponds to the average between both traces. (b) Same as in (a) but for $T = 1.5$ K. Notice the emergence of sharp peaks in $\tau(\theta)$ (red arrows) for θ close to 90° resulting from the intrinsic pinning by the planar structure.

nearly all Fe-based superconductors, see Refs. 9 and 16). Our unpublished transport measurements in $LaFe_{1-x}Co_xAsO$ indicate a very similar T dependence for $\gamma_H = H_{c2}^{ab}/H_{c2}^{c}$.

Figures 7(c) and 7(d) show the field dependencies of γ and n_s for $T = 10$ K. Here γ increases by nearly a factor of 2, from ∼8 at small fields to ∼15 at $H = 18$ T. On the other hand, n_s remains nearly constant in fields up to $H_v = 8$ T, and then decreases at higher fields, extrapolating to $n_s = 0$ at $H(10\,\text{K}) \approx 25$ T. The complete suppression of n_s at this value is consistent with our previous estimate of $\eta H_{c2} \approx 27$ T obtained above. The suppression of $n_s(H)$ upon application of magnetic field is consistent with the onset of orbital pair-breaking by circulating vortex currents as the spacing between the vortex cores becomes smaller than $\approx\sqrt{3}$ of the vortex spacing at H_{c2} where superconductivity is fully suppressed. For instance, the single-band Ginzburg-Landau theory predicts $\lambda^{-2} \propto n_s(H) \simeq n_s(0)(1 - H/H_{c2})$ for T close to T_c.[32] Interestingly, the ratio $H_v/H_{c2} \simeq 1/3$ turned out to be approximately equal to the ratio of the superconducting gaps on the electron and hole pockets of the Fermi surface as observed in Ref. 26. Around $H = 6$–7 T, there is a spike in λ and/or a dip in n_s, the origin of which remains unclear.

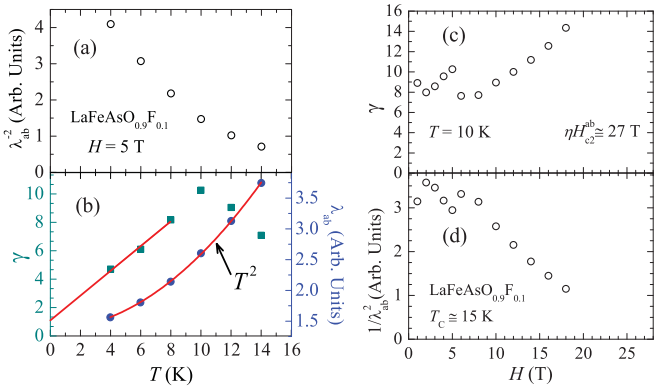

FIG. 7. (Color online) (a) Temperature dependence of the superfluid density $n_s \propto \lambda_{ab}^{-2}$ extracted from the torque data at $H = 5$ T. (b) Temperature dependence of both γ (clear blue markers) and λ_{ab} (blue markers). Here $\lambda_{ab}(T)$ exhibits a quadratic dependence on T. (c) γ as a function of magnetic field as extracted from the fittings in Fig. 2(b). (d) The superfluid density $n_s \propto \lambda_{ab}^{-2}$ as a function of H at $T = 10$ K.

We described our data using the simplest Eq. (1) for the torque in a uniaxial superconductor, assuming that the angular dependencies of λ and ξ are controlled by the single anisotropy parameter γ. A more complicated expression for τ with two different anisotropy parameters $\gamma_H = H_{c2}^{ab}/H_{c2}^{c}$ and $\gamma_\lambda = \lambda_{ab}/\lambda_c$ was suggested for multiband superconductors.[33] However, given that the formula for τ of Ref. 33 was obtained on phenomenological grounds, and the angular dependencies of $\lambda(\theta)$ and $H_{c2}(\theta)$ derived from the multiband BCS theory are much more complicated,[34] we believe that the use of that expression for τ with different γ_H and γ_λ may not unambiguously reveal any new physics as compared to the simpler Eq. (1). Indeed, the fit of our data with τ from Ref. 33 gave behaviors qualitatively similar to those shown above: $\gamma_H \simeq 10\,|_{T\approx T_c}$ increases to a maximum value of 18 before decreasing to much lower values as $T \to 0$. Meanwhile $\gamma_\lambda = 1.4\,|_{T\approx T_c}$ exhibits a mild decrease toward 1 as $T \to 0$. This common tendency of γ to approach a value close to 1 upon decreasing T, observed on many Fe-based superconductors, indicates the increasing contribution of the Pauli pair-breaking effects at lower T's which is taken into account neither in Eq. (1) nor in the expression for τ of Ref. 33.

In conclusion, we report the torque measurements of reversible magnetization of $LaO_{0.9}F_{0.1}FeAs$ single crystals from which the field-dependent mass anisotropy parameter γ and the reduced London penetration depth $\lambda(H,T)/\lambda(0,T)$ were measured. The significant field dependencies of γ and $\lambda(H,T)/\lambda(0,T)$ are consistent with multiband pairing while the observed quadratic temperature dependence of $\lambda(H,T)/\lambda(0,T)$ at low and intermediate T is consistent with the $s^{\pm}$ pairing with interband impurity scattering.

ACKNOWLEDGMENTS

We acknowledge S. Weyeneth for the SQUID measurements. The NHMFL is supported by NSF through Grant No. NSF-DMR-0084173 and the State of Florida. L.B. is supported by DOE-BES through Award No. DE-SC0002613. Work at ETH was supported by the Swiss National Science Foundation and the NCCR program MaNEP.

*Current address: Old Dominion University Department of Physics, 4600 Elkhorn Avenue Norfolk, VA 23529-0116.

†balicas@magnet.fsu.edu

[1] Y. Kamihara, T. Watanabe, M. Hirano, and H. Hosono, J. Am. Chem. Soc. **130**, 3296 (2008); H. Takahashi, K. Igawa, K. Arii, Y. Kamihara, M. Hirano, and H. Hosono, Nature (London) **453**, 376 (2008); X. H. Chen, T. Wu, G. Wu, R. H. Liu, H. Chen, and D. F. Fang, *ibid.* **453**, 761 (2008).

[2] G. F. Chen, Z. Li, D. Wu, G. Li, W. Z. Hu, J. Dong, P. Zheng, J. L. Luo, and N. L. Wang, Phys. Rev. Lett. **100**, 247002 (2008).

[3] Y. Takabayashi, M. T. McDonald, D. Papanikolaou, S. Margadonna, G. Wu, R. H. Liu, X. H. Chen, and K. Prassides, J. Am. Chem. Soc. **130**, 9242 (2008).

[4] C. de la Cruz, Q. Huang, J. W. Lynn, Jiying Li, W. Ratcliff II, J. L. Zarestky, H. A. Mook, G. F. Chen, J. L. Luo, N. L. Wang, and P. C. Dai, Nature (London) **453**, 899 (2008).

[5] I. I. Mazin, D. J. Singh, M. D. Johannes, and M. H. Du, Phys. Rev. Lett. **101**, 057003 (2008).

[6] T. Y. Chen, Z. Tesanovic, R. H. Liu, X. H. Chen, and C. L. Chien, Nature (London) **453**, 1224 (2008).

[7] L. Malone, J. D. Fletcher, A. Serafin, A. Carrington, N. D. Zhigadlo, Z. Bukowski, S. Katrych, and J. Karpinski, Phys. Rev. B **79**, 140501(R) (2009).

[8] H. Ding, P. Richard, K. Nakayama, K. Sugawara, T. Arakane, Y. Sekiba, A. Takayama, S. Souma, T. Sato, T. Takahashi, Z. Wang, X. Dai, Z. Fang, G. F. Chen, J. L. Luo, and N. L. Wang, Europhys. Lett. **83**, 47001 (2008).

[9] F. Hunte, J. Jaroszynski, A. Gurevich, D. C. Larbalestier, R. Jin, A. S. Sefat, M. A. McGuire, B. C. Sales, D. K. Christen, and D. Mandrus, Nature (London) **453**, 903 (2008).

[10] S. Weyeneth, R. Puzniak, U. Mosele, N. D. Zhigadlo, S. Katrych, Z. Bukowski, J. Karpinski, S. Kohout, J. Roos, and H. Keller, J. Supercond. Nov. Magn. **22**, 325 (2009); S. Weyeneth, R. Puzniak, N. D. Zhigadlo, S. Katrych, Z. Bukowski, J. Karpinski, and H. Keller, *ibid.* **22**, 347 (2009).

[11] K. Hashimoto, T. Shibauchi, T. Kato, K. Ikada, R. Okazaki, H. Shishido, M. Ishikado, H. Kito, A. Iyo, H. Eisaki, S. Shamoto, and Y. Matsuda, Phys. Rev. Lett. **102**, 017002 (2009).

[12] P. Popovich, A. V. Boris, O. V. Dolgov, A. A. Golubov, D. L. Sun, C. T. Lin, R. K. Kremer, and B. Keimer, Phys. Rev. Lett. **105**, 027003 (2010).

[13] C. Martin, R. T. Gordon, M. A. Tanatar, H. Kim, N. Ni, S. L. Bud'ko, P. C. Canfield, H. Luo, H. H. Wen, Z. Wang, A. B. Vorontsov, V. G. Kogan, and R. Prozorov, Phys. Rev. B **80**, 020501(R) (2009).

[14] K. Haule, J. H. Shim, and G. Kotliar, Phys. Rev. Lett. **100**, 226402 (2008); Q. Si and E. Abrahams, *ibid.* **101**, 076401 (2008).

[15] P. A. Lee and X. G. Wen, Phys. Rev. B **78**, 144517 (2008).

[16] Y. J. Jo, J. Jaroszynski, A. Yamamoto, A. Gurevich, S. C. Riggs, G. S. Boebinger, D. Larbalestier, H. H. Wen, N. D. Zhigadlo, S. Katrych, Z. Bukowski, J. Karpinski, R. H. Liu, H. Chen, X. H. Chen, and L. Balicas, Physica C **469**, 566 (2009); J. Jaroszynski, S. C. Riggs, F. Hunte, A. Gurevich, D. C. Larbalestier, G. S. Boebinger, F. F. Balakirev, A. Migliori, Z. A. Ren, W. Lu, J. Yang, X. L. Shen, X. L. Dong, Z. X. Zhao, R. Jin, A. S. Sefat, M. A. McGuire, B. C. Sales, D. K. Christen, and D. Mandrus, Phys. Rev. B **78**, 064511 (2008).

[17] M. Angst, R. Puzniak, A. Wisniewski, J. Jun, S. M. Kazakov, J. Karpinski, J. Roos, and H. Keller, Phys. Rev. Lett. **88**, 167004 (2002); A. V. Sologubenko, J. Jun, S. M. Kazakov, J. Karpinski, and H. R. Ott, Phys. Rev. B **65**, 180505(R) (2002); S. L. Bud'ko and P. C. Canfield, *ibid.* **65**, 212501 (2002).

[18] R. Cubitt, M. R. Eskildsen, C. D. Dewhurst, J. Jun, S. M. Kazakov, and J. Karpinski, Phys. Rev. Lett. **91**, 047002 (2003); M. Angst, D. Di Castro, D. G. Eshchenko, R. Khasanov, S. Kohout, I. M. Savic, A. Shengelaya, S. L. Bud'ko, P. C. Canfield, J. Jun, J. Karpinski, S. M. Kazakov, R. A. Ribeiro, and H. Keller, Phys. Rev. B **70**, 224513 (2004).

[19]M. Tegel, S. Johansson, V. Weiss, I. Schellenberg, W. Hermes, R. Pottgen, and D. Johrendt, Europhys. Lett. **84**, 67007 (2008).
[20]V. G. Kogan, Phys. Rev. B **24**, 1572 (1981).
[21]N. D. Zhigadlo, S. Katrych, Z. Bukowski, and J. Karpinski, J. Phys. Condens. Matter **20**, 342202 (2008).
[22]H. Kim, C. Martin, M. E. Tillman, S. K. Kim, S. L. Budko, P. C. Canfield, M. A. Tanatar, and R. Prozorov, Physica C **470**, S363 (2010).
[23]C. J. van der Beek, G. Rizza, M. Konczykowski, P. Fertey, I. Monnet, T. Klein, R. Okazaki, M. Ishikado, H. Kito, A. Iyo, H. Eisaki, S. Shamoto, M. E. Tillman, S. L. Bud'ko, P. C. Canfield, T. Shibauchi, and Y. Matsuda, Phys. Rev. B **81**, 174517 (2010).
[24]H. Luetkens, H. H. Klauss, M. Kraken, F. J. Litterst, T. Dellmann, R. Klingeler, C. Hess, R. Khasanov, A. Amato, C. Baines, M. Kosmala, O. J. Schumann, M. Braden, J. Hamann-Borrero, N. Leps, A. Kondrat, G. Behr, J. Werner, and B. Büchner, Nature Mater. **8**, 305 (2009).
[25]G. Li, G. Grissonnanche, B. S. Conner, L. Balicas *et al*. (unpublished).
[26]C. Martin, M. E. Tillman, H. Kim, M. A. Tanatar, S. K. Kim, A. Kreyssig, R. T. Gordon, M. D. Vannette, S. Nandi, V. G. Kogan, S. L. Bud'ko, P. C. Canfield, A. I. Goldman, and R. Prozorov, Phys. Rev. Lett. **102**, 247002 (2009).
[27]K. Hashimoto, T. Shibauchi, T. Kato, K. Ikada, R. Okazaki, H. Shishido, M. Ishikado, H. Kito, A. Iyo, H. Eisaki, S. Shamoto, and Y. Matsuda, Phys. Rev. Lett. **102**, 017002 (2009).
[28]J. D. Fletcher, A. Serafin, L. Malone, J. G. Analytis, J.-H. Chu, A. S. Erickson, I. R. Fisher, and A. Carrington, Phys. Rev. Lett. **102**, 147001 (2009).
[29]A. V. Chubukov, M. G. Vavilov, and A. B. Vorontsov, Phys. Rev. B **80**, 140515(R) (2009).
[30]A. B. Vorontsov, M. G. Vavilov, and A. V. Chubukov, Phys. Rev. B **79**, 140507(R) (2009).
[31]R. T. Gordon, H. Kim, M. A. Tanatar, R. Prozorov, and V. G. Kogan, Phys. Rev. B **81**, 180501(R) (2010).
[32]E. H. Brandt, Rep. Prog. Phys. **58**, 1465 (1995).
[33]V. G. Kogan, Phys. Rev. Lett. **89**, 237005 (2002).
[34]A. Gurevich, Phys. Rev. B **82**, 184504 (2010); **67**, 184515 (2003); A. A. Golubov and A. E. Koshelev, *ibid*. **68**, 104503 (2003).